Designing and Building a Deep Imaging Multi-Parametric Optical Coherence Tomography System for Disease Assessment

Bruce Vagt, Matthew Foster, Dr. Richard Blackmon

Abstract— **Early cancer detection remains an important problem in healthcare today. Since the mid-1990s, Optical Coherence Tomography (OCT) has been explored as a cancer detection instrument. Previous studies have shown connections between tissue porosity, cell behavior, cell topology, and their relation to cancer and disease progression. Previous researchers have found that in a healthy cell, the pore size of the surrounding extracellular matrix (ECM) is homogenous. However, in a cancerous cell, heterogeneous pores appear. Additionally, as cancer progresses, pore size decreases. Herein, we propose a new method of improving cancer detection using OCT. In a study utilizing an artificial ECM, a connection between pore size and gold nanorod (GNR) diffusion was established such that smaller pores lead to less diffusion, and vice versa. Cell behavior is measured by cell motility, which refers to the rapid, in-place motions of intracellular parts that can be used to assess cell response to therapy, their surrounding environment, and potentially reveal premalignant behavior. Previous investigators have defined two metrics of cell movement, alpha, and motility, which correspond to signal auto-decorrelation and signal amplitude, respectively. Cell topology refers to the 3D structure and shape of cells and cell clusters, which has been shown to mutate in diseases such as cancer. By quantifying cell topology, cellular health can be examined. Techniques using OCT have also been used to monitor the response of diseased tissue to treatment. These studies have been largely independent of each other, and the need for a more holistic measuring system has been called for. This research aims to create a custom OCT system capable of obtaining these metrics simultaneously and with improved imaging depth and comparable resolution. Through an integration of a near-infrared (NIR) laser, interferometer, and LabVIEW control of the system, a new Deep-Imaging, Multi-Parameter OCT (DIMP-OCT) is being created. The system bodes a 4.6µm resolution and 5.4mm imaging depth. This is made possible by a 50-50 fiber optic beam splitter using a 1300nm wavelength laser with 160nm bandwidth, and 2048-pixel spectrometer with a 140kHz linerate. Here, we report the design of the system being built, the techniques used to build and test the hardware, and the approach to developing the graphical user interface. We also will report results from tests to assess DIMP-OCT subsystems.**

I. INTRODUCTION

Cancer is a disease characterized by uncontrollable growth of abnormal or damaged cells, and is one of the leading causes of death in the world[1]. In 2020, approximately 600,000 people died of cancer in the US, and the estimated global death toll was 10 million[2,3]. Previous investigators have shown tissue mechanics change when diseased, apparent in breast cancer[4,5], and play a vital role in drive cancer progression[6,7], yet our understanding is limited due to conflicting studies. Some studies show tissue porosity driving tumor invasion[8,9], while others do not[10]. Being able to quantify and visualize tissue mechanics and cell behavior together has the potential for bridging the gap in our understanding of the complex relationship between these two cancer-driving properties[11,12]. Previous investigators have shown OCT to be capable of quantifying the morphology of cells and cell clusters[13], the size of pores in biological tissue[14], the movement of cells and cell organelles[15,16,17], and the response of diseased tissue to therapy[18]. These studies were conducted independently of each other; therefore, combining these techniques has the potential to reveal the interconnective nature of cell behavior and tissue mechanics to better understand cancer growth and its real-time response to cancer therapies, which will be invaluable in both research and the clinic.

Current gold standards in cancer assessment are invasive and destructive, limiting the ability to research and understand the nature of diseased tissue. Additionally, results have a time delay of a few days to a week or more. Thus, a non-invasive, non-destructive, real-time imaging system would be a great advancement in disease assessment. OCT is a subsurface laser-based imaging technique that functions similarly to ultrasound; however, instead of sound waves, light waves are used, allowing images to be taken on the micron to millimeter scale with high resolution. Additionally, OCT has already been shown to be capable of real-time image display. Thus, OCT is a prime candidate for a non-invasive, disease assessment system. As of 2023, off shelf OCT systems can range from $74,000 to $91,000. This project aims to build and test an OCT medical imaging system capable of simultaneously obtaining the aforementioned metrics for a fraction of the cost of an off-shelf system, all with comparable functionality and enhanced imaging capabilities.

II. INSTRUMENT DESIGN

DIMP-OCT has two fundamental components: deep imaging and multi-parameter acquisition. The capability for OCT to measure multiple parameters simultaneously is not dependent on hardware of the system, but rather from the

*Research supported by Elon University.
Bruce Vagt is with Elon University, Elon, NC 27244 USA
Matthew Foster, Founder of Motorboat Mechanics, Raleigh, NC USA
Dr. Richard Blackmon, is with Elon University, Elon, NC 27244 USA. (phone: (336) 278-6784; e-mail: rblackmon2@elon.edu).

processing of the image after collection. Imaging depth and resolution, however, are dependent on the system components, such that hardware can be selected to enhance both simultaneously according to the following equations.

Axial resolution is a defined by the coherence length of the light source, and is therefore dependent on the center wavelength and limited by the spectral bandwidth.

$$\Delta z = \frac{2\ln(2)}{\pi} * \frac{{\lambda_c}^2}{\Delta\lambda} \quad (1)$$

Later resolution is limited by the spot size of the focused probing beam, and is a function of focal length, center wavelength, and beam diameter. Our system uses a beam diameter of 1-2 mm

$$\Delta x = \frac{4\lambda_c}{\pi}\frac{f}{d} \quad (2)$$

Max imaging depth is limited by either number of pixels recorded or spectral bandwidth, and is a function of center wavelength, light source bandwidth, and number of pixels recorded. We record 2048 pixels.

$$z_{max} = \frac{1}{4}\frac{{\lambda_c}^2}{\frac{\Delta\lambda}{N}} \quad (3)$$

According to previous investigations[19], as wavelength increases signal attenuation decreases resulting in improved image clarity. Coupled with a 140kHz linerate camera, the use of a 1300nm wavelength laser allows for high resolution, deep imaging capability.

A. Hardware

The hardware, *Figure 1*, has key components of a broadband light source, 50-50 fiber optic beam splitter as an interferometer, a retroreflector, a line rate camera, and Data Acquisition System (DAQ) controlled galvo mirrors. An optical interferometer is a measurement tool that splits a coherent light source though a half-silvered mirror and combines the light waves to create an interference pattern. OCT utilizes a spatially resolved interference pattern to collect measurements. It does so use a 50/50 beam splitter that employs a reference arm and sample arm to create the interference pattern, and once the reference image is subtracted from the sample image, the remaining image data represents subsurface structures. A galvanometer system with silver coated mirrors is used to steer the sampling light beam to different positions on the sample based on a voltage level provided from the LabVIEW interface, the equation for this is shown in LabVIEW code in *Figure 4***.** The galvo mirrors play a pivotal role in data acquisition as they allow for highly precise positioning on the sample, as well as acquisition in a straight line to create a 2D image known as a B-scan. Some challenges encountered when building the system include optical alignment, improper equipment, and equipment troubleshooting. A particularly difficult piece of equipment for this research was the Cobra 1300 Spectrometer). Some challenges for the camera stemmed from the goal of controlling the camera's frame rate and exposure time as these are controlled by internal settings, and not directly adjustability with LabVIEW functions.

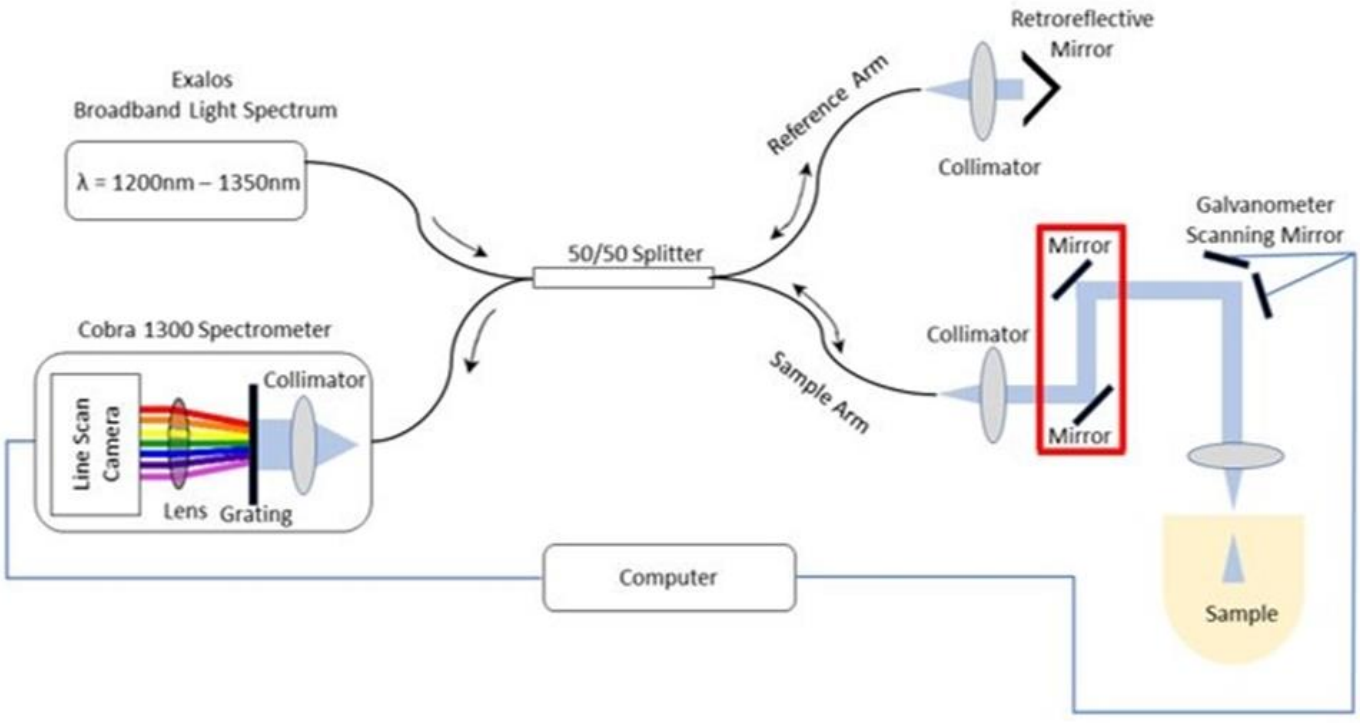

Figure 1. Schematic of fiber-based DIMP-OCT

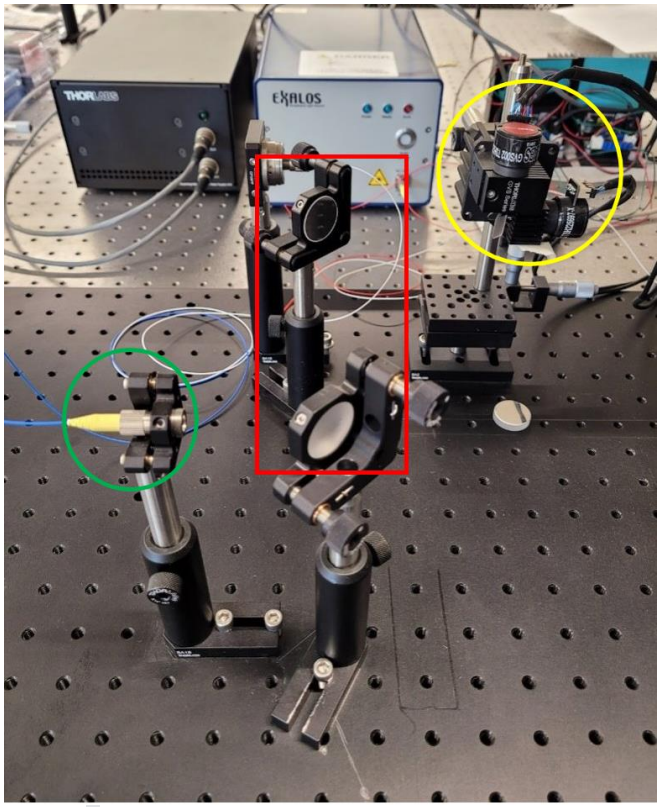

Figure 2. Hardware for interferometer, including periscope (red box), galvo system (yellow circle), and sampling arm (green circle)

TABLE I. DIMP-OCT HARDWARE AND SPECIFICATIONS

Hardware	Specs	Vendor	Model #
Light Source	Wavelength: 1280nm Power: 15mW Bandwidth: 3dB (145nm) 10db (180nm)	Exalos	EBS300045-02
Interferometer	Dual wavelength 1310nm & 1550nm 50-50 ratio splitter	ThorLabs	10202A-50-FC
DAQ	Max voltage: 10V	NI	150199E-01L
Galvo system w/ silver coated mirrors	Small <5mm diameter beams. 12.5deg scan angle (.8v per deg)	Thorlabs	GVS002
Cobra 1300 Spectrometer	Pixels: 2048, Max linerate:147kHz, BW: 245nm, Spectral Res.: 0.12nm	Wasatch Photonics	C1300-1300/245/147-SG2K
Reference arm retroreflector	AR coating: 1050nm-1700nm	Thorlabs	PS975M-C

B. Software

The OCT system runs using NI-LabVIEW software, Figure 3 shows the graphical user interface (GUI) used for DIMP-OCT and the laser spectrum recorded using the GUI. When designing the GUI, the primary consideration of user-friendliness, because the ultimate objective of OCT is to be used in clinical settings. This means the system needs to be simple and easy to navigate so that clinicians can quickly and accurately take measurements and provide a diagnosis. To achieve this simplicity, subVIs were utilized which are analogous to functions in scripting languages. This allows for a clean interface and cleaner code but increases the complexity of troubleshooting somewhat as the code now has layers which must all work in concert for effective execution. Additionally, the GUI allows for control over displayed images properties (an upgrade from previous iterations), enabling users to adjust parameters such as contrast for brighter images. Some software challenges encountered include real-time display, subVI integration, and control over internal camera settings.

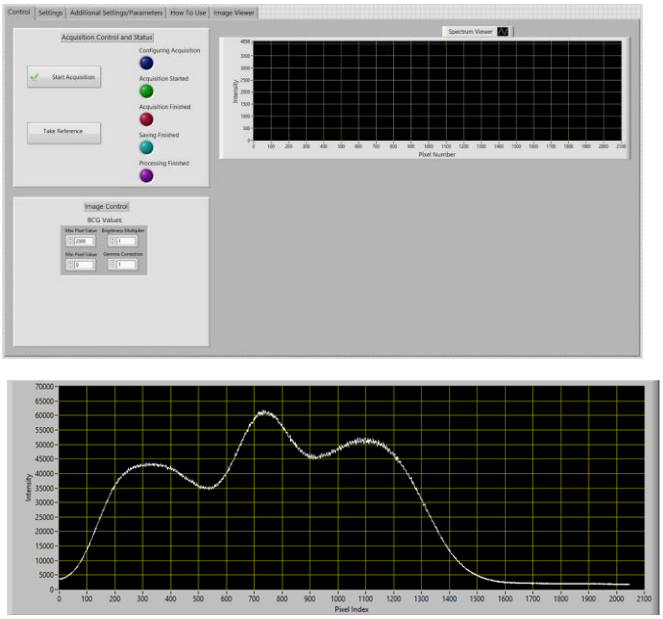

Figure 3. Graphical User Interface (GUI), main window (top); Spectrum measured using a Cobra 1300 Spectrometer (bottom). The x-axis represents the pixel number of the camera (corresponds to light wavelength), and y-axis the intensity of light measured from that pixel.

C. System Utility

In a study using Diffusion-Sensitive OCT (DS-OCT), it was found that GNR diffusion is positively correlated with tissue pore size[14]. In cancer, the ECM becomes heterogeneous and dense resulting in decreased pore size, thus provided a metric for disease assessment based on GNR diffusion. Another study investigated the intracellular motion of mammary epithelial cells and created metrics alpha and motility to characterize these motions. Investigators found that motility and alpha were sensitive to cell health, making the metrics valuable for studying disease progression and treatments[15]. DIMP-OCT is both diffusion sensitive and capable of measuring Motility and alpha, allowing it to assess ECM and potentially cellular health, allowing for a holistic assessment of tissue health. These capabilities will be built into the normal operation of the system so that investigators can monitor ECM- and cell-sensitive metrics in real-time for rapid assessment of diseased tissue.

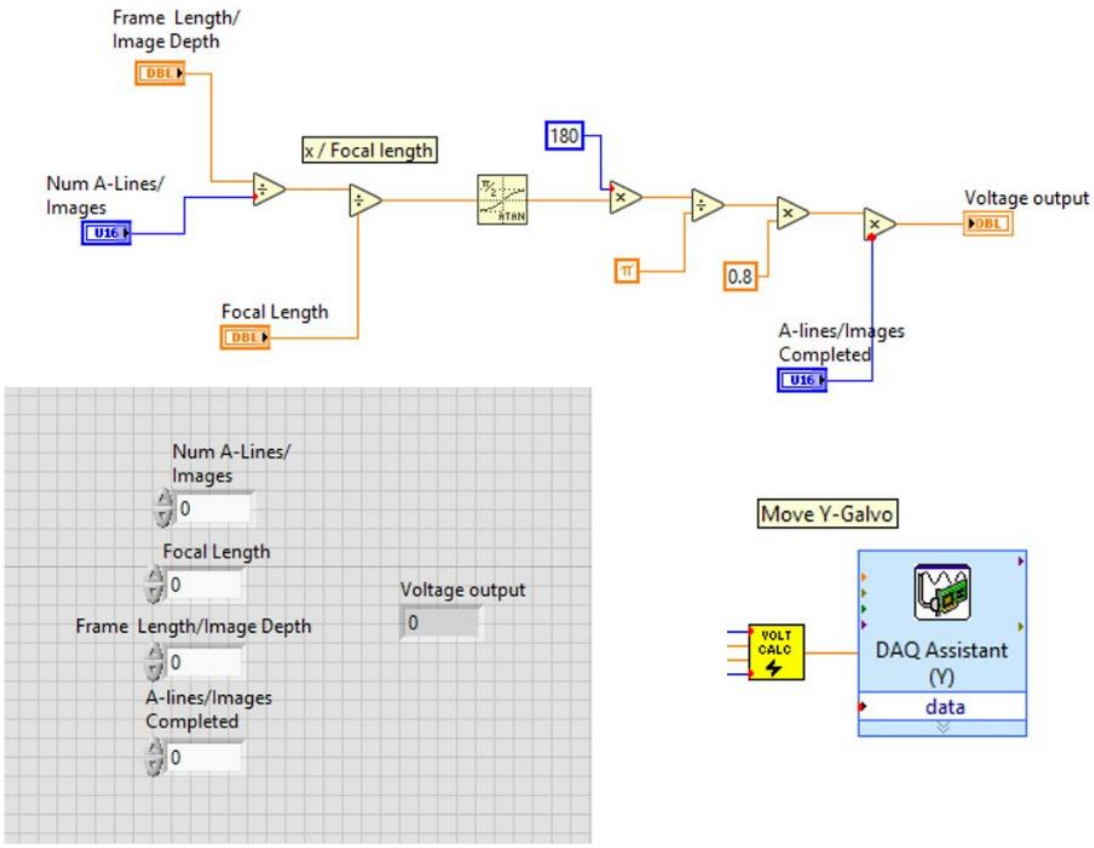

Figure 4. LabView block diagram of subVI, corresponding front page, and use of subVI

D. Future Directions

Although the system is capable of operating, there is still work to be done in order for it to be capable of disease assessment. The system is not in optical alignment as lab locations have changed since last use, so work is being done to realign the system. Previous iterations of the system used a DAQ with a max voltage of 5V limiting the max scanning angle of the galvo system below their operational max. A new DAQ with a max voltage of 10V has been procured and is in process of being integrated with the system allowing for use of the galvo system's full potential. Currently, image processing algorithms for metrics of diffusion, motility, and alpha are utilized in post using MATLAB, thus limiting the potential for real-time image display that could be clinically relevant. Therefore, work is being done to incorporate data processing algorithms into the system's LabVIEW code.

III. Conclusion

In conclusion, the proposed DIMP-OCT will allow for simultaneously measurement of tissue porosity, cell behavior, and cell topology, resulting in a more holistic measurement of human tissue health, making it a promising candidate for disease assessment and monitoring. The integration of a NIR light source and interferometer provides deeper imaging without sacrificing resolution. This system will hopefully become a powerful tool to enable accurate disease assessment and treatment monitoring.

Acknowledgment

We acknowledge Alexandre Hebert and Brittany Barton for their previous work on this research project.

References

[1] "What Is Cancer? - NCI," Sep. 17, 2007. https://www.cancer.gov/about-cancer/understanding/what-is-cancer (accessed Apr. 02, 2023).
[2] "Cancer." https://www.who.int/news-room/fact-sheets/detail/cancer (accessed Apr. 02, 2023).
[3] "Cancer Facts & Figures 2020 | American Cancer Society." https://www.cancer.org/research/cancer-facts-statistics/all-cancer-facts-figures/cancer-facts-figures-2020.html (accessed Apr. 02, 2023).
[4] Falzon G, Pearson S, Murison R. Analysis of collagen fibre shape changes in breast cancer. Phys Med Biol. 2008 Dec 7;53(23):6641-52. doi: 10.1088/0031-9155/53/23/001. Epub 2008 Nov 7. PMID: 18997272.
[5] Luo H, Tu G, Liu Z, Liu M. Cancer-associated fibroblasts: a multifaceted driver of breast cancer progression. Cancer Lett. 2015 Jun 1;361(2):155-63. doi: 10.1016/j.canlet.2015.02.018. Epub 2015 Feb 17. PMID: 25700776.
[6] Cox TR, Erler JT. Remodeling and homeostasis of the extracellular matrix: implications for fibrotic diseases and cancer. Dis Model Mech. 2011

Mar;4(2):165-78. doi: 10.1242/dmm.004077. Epub 2011 Feb 14. PMID: 21324931; PMCID: PMC3046088.
[7] Barcus CE, Keely PJ, Eliceiri KW, Schuler LA. Stiff collagen matrices increase tumorigenic prolactin signaling in breast cancer cells. J Biol Chem. 2013 May 3;288(18):12722-32. doi: 10.1074/jbc.M112.447631. Epub 2013 Mar 24. PMID: 23530035; PMCID: PMC3642318.
[8] Guzman A, Ziperstein MJ, Kaufman LJ. The effect of fibrillar matrix architecture on tumor cell invasion of physically challenging environments. Biomaterials. 2014 Aug;35(25):6954-63. doi: 10.1016/j.biomaterials.2014.04.086. Epub 2014 May 15. PMID: 24835043.
[9] Wolf K, Te Lindert M, Krause M, Alexander S, Te Riet J, Willis AL, Hoffman RM, Figdor CG, Weiss SJ, Friedl P. Physical limits of cell migration: control by ECM space and nuclear deformation and tuning by proteolysis and traction force. J Cell Biol. 2013 Jun 24;201(7):1069-84. doi: 10.1083/jcb.201210152. PMID: 23798731; PMCID: PMC3691458.
[10] Zaman MH, Trapani LM, Sieminski AL, Mackellar D, Gong H, Kamm RD, Wells A, Lauffenburger DA, Matsudaira P. Migration of tumor cells in 3D matrices is governed by matrix stiffness along with cell-matrix adhesion and proteolysis. Proc Natl Acad Sci U S A. 2006 Jul 18;103(29):10889-94. doi: 10.1073/pnas.0604460103. Epub 2006 Jul 10. Erratum in: Proc Natl Acad Sci U S A. 2006 Sep 12;103(37):13897. PMID: 16832052; PMCID: PMC1544144.
[11] Baghban R, Roshangar L, Jahanban-Esfahlan R, Seidi K, Ebrahimi-Kalan A, Jaymand M, Kolahian S, Javaheri T, Zare P. Tumor microenvironment complexity and therapeutic implications at a glance. Cell Commun Signal. 2020 Apr 7;18(1):59. doi: 10.1186/s12964-020-0530-4. PMID: 32264958; PMCID: PMC7140346.
[12] Winkler J, Abisoye-Ogunniyan A, Metcalf KJ, Werb Z. Concepts of extracellular matrix remodelling in tumour progression and metastasis. Nat Commun. 2020 Oct 9;11(1):5120. doi: 10.1038/s41467-020-18794-x. PMID: 33037194; PMCID: PMC7547708.
[13] Chhetri RK, Phillips ZF, Troester MA, Oldenburg AL. Longitudinal study of mammary epithelial and fibroblast co-cultures using optical coherence tomography reveals morphological hallmarks of pre-malignancy. PLoS One. 2012;7(11):e49148. doi: 10.1371/journal.pone.0049148. Epub 2012 Nov 12. PMID: 23152864; PMCID: PMC3495770.
[14] Blackmon RL, Sandhu R, Chapman BS, Casbas-Hernandez P, Tracy JB, Troester MA, Oldenburg AL. Imaging Extracellular Matrix Remodeling In Vitro by Diffusion-Sensitive Optical Coherence Tomography. Biophys J. 2016 Apr 26;110(8):1858-1868. doi: 10.1016/j.bpj.2016.03.014. PMID: 27119645; PMCID: PMC4850325.
[15] Oldenburg AL, Yu X, Gilliss T, Alabi O, Taylor RM 2nd, Troester MA. Inverse-power-law behavior of cellular motility reveals stromal-epithelial cell interactions in 3D co-culture by OCT fluctuation spectroscopy. Optica. 2015 Oct 20;2(10):877-885. doi: 10.1364/OPTICA.2.000877. Epub 2015 Oct 9. PMID: 26973862; PMCID: PMC4783137.
[16] Liu Z, Kurokawa K, Hammer DX, Miller DT. *In vivo* measurement of organelle motility in human retinal pigment epithelial cells. Biomed Opt Express. 2019 Jul 19;10(8):4142-4158. doi: 10.1364/BOE.10.004142. PMID: 31453000; PMCID: PMC6701538.
[17] Arezza NJJ, Razani M, Kolios MC. Dynamic light scattering optical coherence tomography to probe motion of subcellular scatterers. J Biomed Opt. 2019 Feb;24(2):1-7. doi: 10.1117/1.JBO.24.2.025002. PMID: 30770677; PMCID: PMC6987633.
[18] Yu X, Fuller AM, Blackmon R, Troester MA, Oldenburg AL. Quantification of the Effect of Toxicants on the Intracellular Kinetic Energy and Cross-Sectional Area of Mammary Epithelial Organoids by OCT Fluctuation Spectroscopy. Toxicol Sci. 2018 Mar 1;162(1):234-240. doi: 10.1093/toxsci/kfx245. PMID: 29140506; PMCID: PMC6059173.
[19] J. M. Schmitt, A. Knuttel, M. Yadlowsky, and M. A. Eckhaus, “Optical-coherence tomography of a dense tissue: statistics of attenuation and backscattering,” *Phys. Med. Biol.*, vol. 39, no. 10, p. 1705, Oct. 1994, doi: 10.1088/0031-9155/39/10/013.